

# Gasification of eucalyptus in downdraft fixed bed to obtain synthesis gas

Roberto Canuto Paiva, Luiz Eduardo Pizarro Borges\*, Fábio Bellot Noronha

Military Institute of Engineering, Praça General Tibúrcio, 80, 22290-270, Praia Vermelha, Rio de Janeiro, RJ, Brazil

\*luiz@ime.eb.br

**ABSTRACT:** Gasification is a process where thermochemical conversion of biomass occurs yielding combustible gas or synthesis gas, depending on reaction circumstances, catalyst use or type of gasifier. The gasifier was fed in batches while air was continuously fed at flow rates between  $5.62 \times 10^{-3}$  mol/s and  $9.96 \times 10^{-3}$  mol/s. Air factors were in the range of 0.41 to 0.48. Mass and energy balances were realized, and thermochemical phenomena in the biomass bed were studied. Gas produced during the gasification process was analyzed every 20 minutes by gas chromatography with a Varian CP 3800 chromatographer equipped with a TCD detector. Peaks of 12.8%  $H_2$  and 14.8% CO and mean fractions of 5.36%  $H_2$  and 6.73% CO were registered at airflow of  $9.96 \times 10^{-3}$  mol/s. The gas produced had a higher heating value of  $1617 \text{ kJ/Nm}^3$  and a lower heating value of  $1491 \text{ kJ/Nm}^3$ .

**KEYWORDS:** Biomass. Eucalyptus. Gasification. Pyrolysis.

**RESUMO:** Gaseificação é o processo em que ocorre a conversão termoquímica da biomassa, gerando gás combustível ou gás de síntese, dependendo das condições reacionais, uso de catalisadores e do tipo de gaseificador utilizado. O gaseificador foi alimentado por batelada e o ar foi alimentado continuamente em vazões que variaram de  $5,62 \times 10^{-3}$  mol/s a  $9,96 \times 10^{-3}$  mol/s e o fator de ar ficou na faixa de 0,41 a 0,48. Balanços de massa, balanço de energia e fenômenos termoquímicos do leito de biomassa foram estudados. Os gases gerados durante o processo de gaseificação foram analisados a cada 20 minutos por cromatografia gasosa, utilizando Cromatógrafo Varian CP 3800 com detector de TCD. Picos de frações de  $H_2$  e CO de até 12,8% e 14,8%, respectivamente, e frações médias de 5,36% de  $H_2$  e 6,73% de CO foram observadas para a vazão de ar de  $9,96 \times 10^{-3}$  mol/s. O gás produzido apresentou um poder calorífico superior de  $1.617 \text{ kJ/Nm}^3$  e um poder calorífico inferior de  $1.491 \text{ kJ/Nm}^3$ .

**PALAVRAS-CHAVE:** Biomassa. Eucalipto. Gaseificação. Pirólise.

## 1. Introduction

The growing concern with the carbon dioxide balance in the atmosphere has been a driving factor in the development of new forms of fuel [1]. In this context, the use of biomass in place of fossil fuels has aroused the interest of government agencies, industry and the scientific community [2]. In addition, biomass is a widely available resource, making it possible to generate energy even in regions with difficult access [3]. Some regions of the Brazilian Amazon are examples of places for which biomass would be a good solution for energy generation. However, modern energy recovery systems require substances with well-defined properties and typically tolerate

low levels of impurities. These latter requirements contrast strongly with the physical and chemical properties of biomass [4].

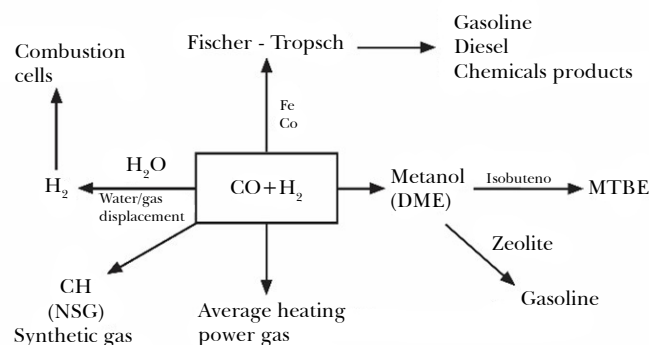


**Fig. 1** – Examples of possibilities for using the synthesis gas. **Source:** Adapted from [5].

Given this context, the transformation of biomass into something more applicable in more refined systems, which require a high level of purity, is expected. Syngas may be the technological solution to this intention. This gas is a mixture of carbon monoxide (CO) and hydrogen (H<sub>2</sub>), presenting great industrial versatility. The applications of this mixture include numerous processes, such as: shift reaction for hydrogen production; Fisher-Tropsch reaction to obtain hydrocarbons; catalytic production of methanol; production of synthetic natural gas (SNG); or direct burning in combustion engines [5]. Fig. 1 presents the application of synthesis gas for energy generation and production of various chemical compounds.

### 1.1 General aspects of gasification

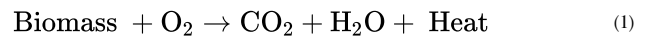
Gasification is a partial oxidation process in which the formation of a gas product with chemical and energetic importance occurs. Oxidizing agents

(or gasifying agents) may vary, but in most processes oxygen, air, water vapor, supercritical water or even carbon dioxide is used [5].

According to Lora *et al.* [5], the gasification process can be separated into two stages: pyrolysis and gasification. The supply of heat is necessary for the pyrolysis step to occur, according to Equation 3. Thus, the biomass must reach a temperature high enough for its decomposition into coal, gases and tar. Fig. 2 illustrates the steps of gasification.

If the gasifying agent is based on O<sub>2</sub>, part of the biomass can be burned (Equations 1 and 2) to provide the heat required for pyrolysis. If the gasifying agents are water vapor or CO<sub>2</sub>, heat must be supplied from an external source for the process to occur.

Combustion of biomass



Combustion of coal

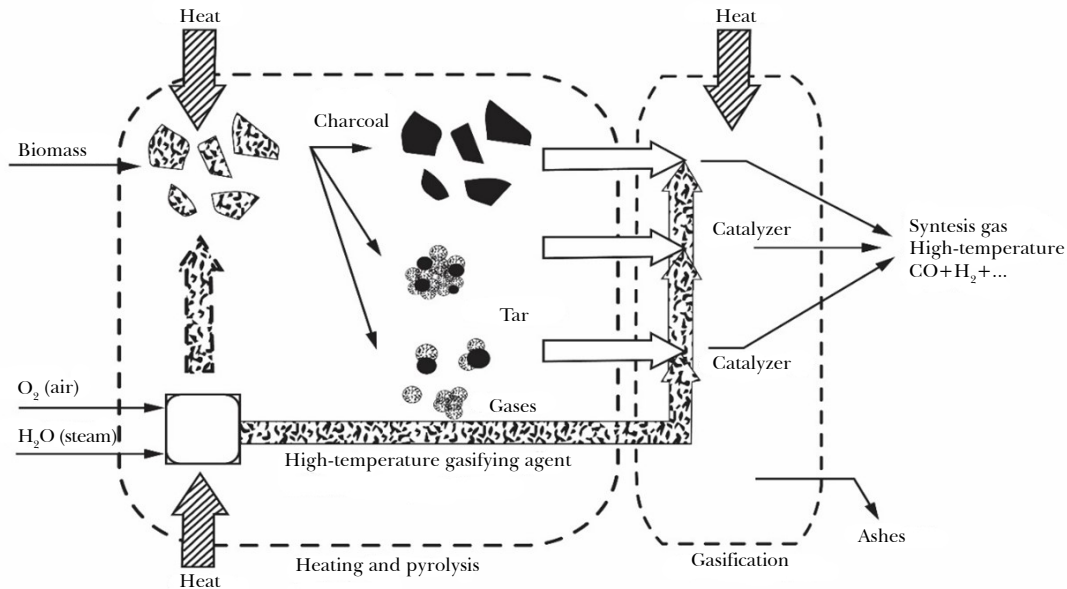
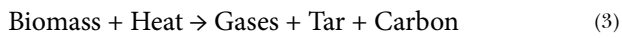


Fig. 2 – Illustration of the steps involved in the gasification process. Source: Adapted from [5].

Following the conception of the gasification process of Lora *et al.* [5], the reactions of the two gasification steps are as follows:

1) Pyrolysis



2) Gasification (Equations 4 to 8) [6, 7, 8]:

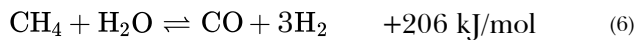
Boudouard's reaction



Methanation



Methane steam reforming



Carbon steam reforming:



Shift reaction water-gas



The occurrence of several reactions causes other products besides CO and H<sub>2</sub> to be present in the synthesis gas. Due to the diverse composition of the raw material and incomplete conversion, biomass gas may contain tar, inorganics (alkali metals, alkaline earth metals, sulfur, chlorine, etc.), and solid particles [9]. Such impurities represent a major obstacle in the use of biomass gas in the processes presented by Fig. 1. Therefore, obtaining syngas free of particles and tar is extremely important in the viability of biomass gasification to obtain energy [10].

## 1.2 Types of gasifier

Lora *et al.* [5] classifies the gasifiers according to the mode of operation, taking into account the direction of gas movement and the nature of the bed. There are two main classes of gasifiers: fixed-bed and fluidized-bed.

### 1.2.1 Fixed-bed gasifiers

The term “fixed-bed” indicates the stationary characteristic of the biomass bed. Although there is a

downward movement due to the consumption of the material to be carbonated, the displacement speed of the solid bed is much lower than the speed of the gases that percolate it. Therefore, the term “fixed-bed” is used, although there is a small mobility of the solid part.

Following the classification of the literature [5], fixed-bed gasifiers can be divided according to the direction of flows, as follows:

a) concurrent flow: both the biomass bed and the gases produced move in the downward direction and the ash is deposited at the bottom of the gasifier. Therefore, the gassing agent is injected into the upper part of the throat where the gassing occurs;

b) countercurrent flow: biomass flows downward as it is consumed, while produced gases flow upward. Therefore, the gasifier agent is injected into the bottom of the gasification throat. The ashes also accumulate at the bottom of the equipment;

c) cross flow: the gasification agent is injected into the side and the effluent gases are collected on the opposite side of the gasifier. As in concurrent and countercurrent gasifiers, ash is deposited on the bottom and the biomass bed moves downward as it is consumed.

Fig. 3 presents a sketch of the fixed-bed gasifiers.

### 1.2.2 Fluidized-bed gasifiers

The fluidized bed gasifiers can be classified according to the mode of operation of the fluidization, as follows [5]:

a) bubbling fluidized-bed: in this type of operation, the gasification agents promote the movement of a particle bed composed of inert material mixed with biomass. The inert can also be replaced by catalytic materials in order to improve the efficiency of the gasification or reduce the impurity content in the effluent gas. In the bubbling bed, solids are not carried out of the pipe where fluidization occurs. Therefore, there is no significant recirculation of bed material. Possible solid impurities carried by the gas may, however, be returned to the bed. In this type of

reactor, normally, there is a region with a larger cross-sectional area where the superficial velocity of the gas is low and causes the particles to settle and not escape at the top;

b) circulating fluidized bed: in this type, an inert or catalytic material mixed with biomass is also used. However, the particle mixture is fluidized and carried through the reactor. Thus, the outlet of the reactor is composed of the mixture of gases and bed particles. The solid material may then be separated by physical methods and returned to the bed, and the produced gas escapes free of solids;

c) fluidized bed entrained: in this case, the finely divided raw material is carried by pneumatic transport to high temperature regions where the gasification process takes place. In this type, inert or catalytic solid particles other than biomass are not used. High temperatures are obtained by oxidizing part of it.

The classification of the fixed bed gasifiers presented is illustrated by Fig. 4.

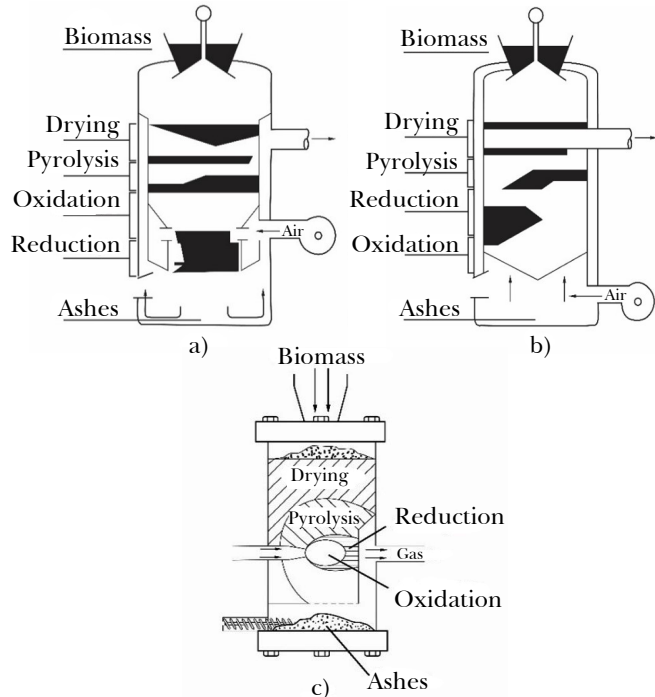


**Fig. 3** – Main types of fixed-bed gasifiers: a) competitor; b) countercurrent; c) cross-flow. **Source:** Adapted from [5].

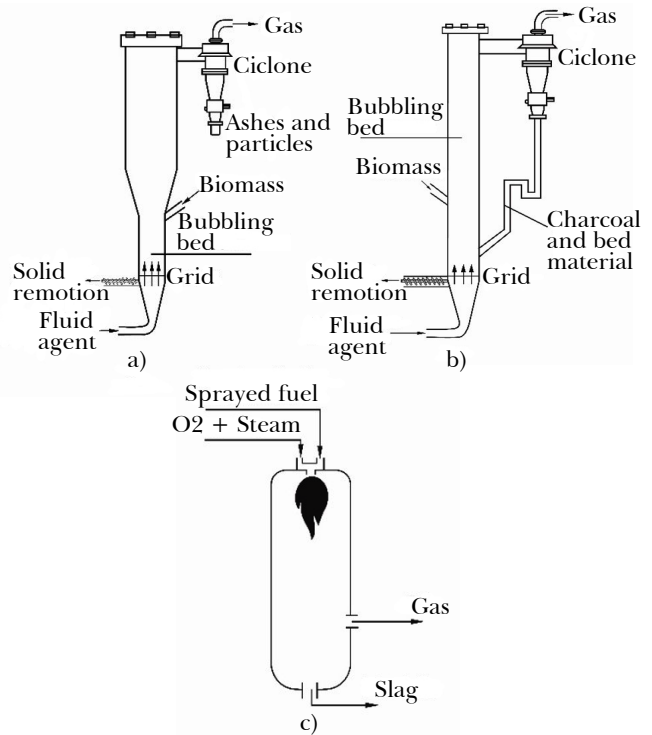


**Fig. 4** – Main types of fluidized bed gasifiers: a) bubbling bed; b) circulating bed; c) example of entrained bed. **Source:** Adapted from [5].

Fluidized bed gasifiers have the advantage of allowing the introduction of a catalytic material, replacing the inert particulate. However, the catalyst must be resistant to both shock and sintering due to the vigorous movement of the bed and the high temperatures employed [9].

The construction of gasifiers is not restricted to the types presented. However, in the vast majority of cases, the variants will more closely resemble some of the models presented.

### 1.2.3 Concurrent fixed bed gasifier (downdraft)

The object of this work is a downdraft gasifier. Fig. 5 presents the typical location of the drying, pyrolysis, combustion and reduction regions for a fixed bed gasifier in concurrent flow, known as a downdraft gasifier.

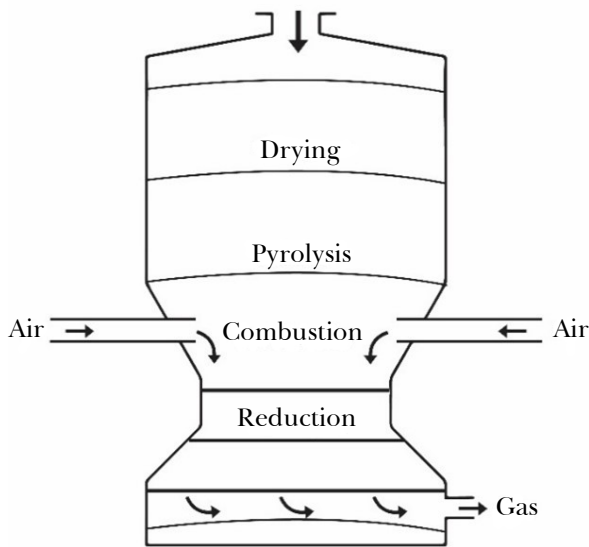
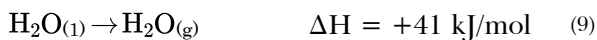


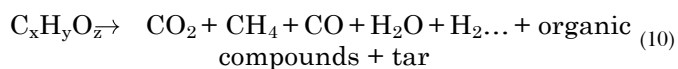
**Fig. 5** – Division and location of gasification subprocesses in a concurrent flow gasifier in a fixed bed (*downdraft*). **Source:** Prepared by the authors.

With respect to the regions presented, the chemical processes that occur in each one for a concurrent fixed bed gasifier are detailed:

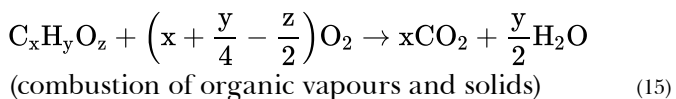
Drying [11]



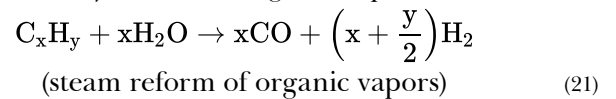
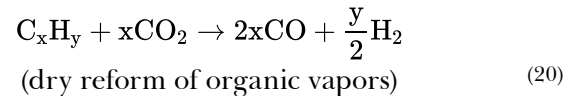
Pyrolysis [12]



Combustion [7, 12]



Reduction [7, 8]



### 1.3 Tar

Tar is a set of substances originated from thermal decomposition or thermo-oxidation of biomass. Its components usually have a high molecular weight (usually heavier than benzene) and a high concentration of aromatic components, which makes it quite thermally stable. Given these characteristics, tar causes problems in the subsequent treatment of syngas. Such problems range from deactivation of catalysts by carbon deposition, to clogging of pipes by condensation and corrosion of surfaces [13].

Milne, Evans and Abatzoglou [10] present the classification for tar from biomass as follows:

a) primary tar: originated directly from the decomposition of the lignocellulosic material;

b) secondary tar: produced from the reactions of primary tar – in this group, olefins and phenolic compounds stand out;

c) tertiary tar: characterized by methylated aromatic compounds such as toluene, methylnaphthalene, xylenes and condensed tertiary, such as polyaromatic hydrocarbons.

Each of these classes has a higher or lower occurrence depending on the level of thermal severity in the gasifier. Primary tars tend to form at lower temperatures (400°C to 650°C); secondary tars, at intermediate temperatures (650°C to 850°C); and tertiary tars are mainly produced from 850°C [10]. Table 1 shows the main substances depending on the formation temperature.

**Table 1** – Main groups of compounds present in the tar.

Pyrolysis temperature (°C)			
450 to 500	600 to 650	700 to 800	900 to 1000
Acids	Benzenes	Naphthalenes	Naphthalenes
Aldehydes	Phenols	Acenaphthyl- lenes	Acenaphthylenes
Ketones	Catechols	Fluorenes	Phenanthrene
Furans	Naphthalenes	Phenanthrene	Fluoranthenes
Alcohols	Biphenyls	Benzaldehyde	Pyrenes
Complex oxygenates	Phenanthrene	Phenols	Acephenanthrylenes
Phenols	Benzofurans	Naphthofurans	Benzanthrene
Guaiacols	Benzaldehyde	Benzanthrene	Benzopyrenes
Syringols			
Complex phenols			

**Source:** Adapted from [10].

Table 2 shows that the removal of tar from the synthesis gas is of crucial importance to enable the use of biomass synthesis gas in chemical processes and energy recovery processes. The gasifiers operate by producing syngas with a tar content in the range of 100 to 100,000 mg/Nm<sup>3</sup> [9], which is well above the permissible values for almost all applications of this gas.

**Table 2** – Limits of tar content for the use of the synthesis gas.

Typical tar content in biomass gas	0,1-100 g/m <sup>3</sup>
<b>Gas application</b>	<b>Maximum acceptable tar content</b>
Steam generation station	Not important, but condensation should be avoided
Gas engine	<100 mg/m <sup>3</sup>
Gas turbine	<50 mg/m <sup>3</sup>
Cast Carbonate Fuel Cell	<2.000 ppmV
Fuel cell with proton	<100 ppmV
Synthesis of Fisher-Tropsch	<1 ppmV

**Source:** Adapted from [9].

## 1.4 Elimination of tar

Considering the difficulties imposed by the presence of tar, its elimination is sought through separation or by its decomposition. Most of the techniques studied involve physical, thermal and catalytic methods. Physical methods focus on tar removal by physical pathways such as condensation, filtration, electrostatic precipitation, cyclone installation,

etc. Thermal methods focus on its degradation by high temperature, causing it to react with other gas components or break down into lighter components. Catalytic methods also seek to destroy tar, but without resorting to thermal levels as severe as those employed by thermal methods [13].

A widely used catalytic method is the steam reforming of tar. This technique has as advantages the degradation of tar, with hydrogen and carbon monoxide as products [13]. Thus, in addition to the elimination of tar, there is an increase in the amount of syngas produced. However, the development of catalysts capable of acting effectively in the steam reforming of tar is still a challenge. High tar conversions have already been obtained with nickel-based catalysts, but the main problem affecting catalyst performance is deactivation, either by carbon deposition or by poisoning [13].

## 1.5 Motivation and objectives

This work is motivated by the importance of the gasification process for the viability of the use of biomass as a source of several products of energy concern. Nevertheless, the need to produce biomass synthesis gas with a high level of purity is also the reason why it is desired to study the gasification process.

The eucalyptus fine brushwood and pointers are residues that have relevant importance in forestry, reaching a production of 17 tons/ha in dry mass. This represents 8.5% of the total mass production of a 7-year eucalyptus forest [14]. Considering that Brazil has approximately 5.7 million hectares planted with eucalyptus [15], it is clear the importance of fine pointers and gallery residues at the national level.

In a complementary way, the study and improvement of the bench gasification unit is fundamental for the development of future work that will focus on the purification of the synthesis gas. Therefore, this work is also motivated by its contribution in allowing future studies in the various areas of tar removal and other impurities.

Given these motivating circumstances, this work aims to study the gasification process of eucalyptus biomass in order to identify potential improvements of the experimental arrangement for synthesis gas production. Nevertheless, it is sought to generate, in the laboratory, a synthesis gas stream with characteristics similar to those that would be obtained industrially and thus enable future studies of conditioning and purification of this gas.

## 2. Material and Methods

The gasification unit was constructed from a bench-scale downdraft fixed-bed gasifier. This gasifier was

sized to meet the production of syngas on a laboratory scale in order to provide means for conditioning research and purification of syngas. Therefore, a gasifier had already been built, but no test had been performed, and no method or analysis mechanism had been installed in the gasifier. Its main dimensions are: internal diameter of 10 cm, total height of 70 cm and air injection point 3 cm above the grid.

Bourdon pressure gauges and volume meters (gas meter from the manufacturer LAO, model G1 for the inlet and model G2.5 for the outlet) were installed at the inlet and outlet of the unit. Type K thermocouples were installed to measure the temperature at the outlet of the gasifier and inside the bed.

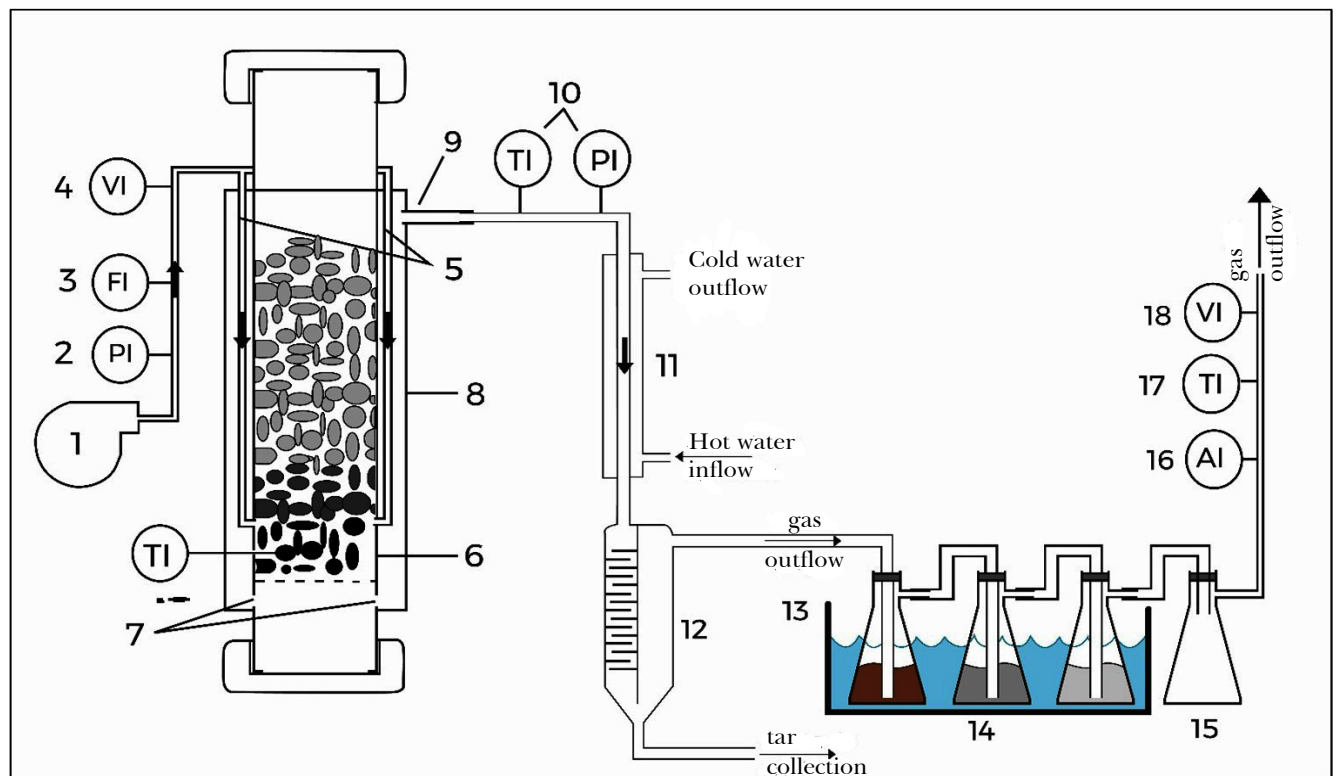


Fig. 6 – Scheme of the assembly for the study of the gasification process. Source: Prepared by the authors.

Preliminary tests revealed that the gas produced could not be analyzed by gas chromatography, since the samples had a high content of vapors that condensed and could damage the equipment. Thus, certain precautions were taken:

- condenser installation;
- installation of a winding stretch to collapse the liquid particles;
- installation of bubblers with isopropanol and trap.

Fig. 6 shows scheme of the gasification unit: the air is supplied by a compressor (1) and fed at the top of the gasifier jacket, passing through the pressure gauges (2), flow (3) and the volume integrator gauge (4). The air flows in the pipeline (5) (without contact with the biomass) countercurrently with the hot effluent gases from the reaction region. The heated air is then injected into the biomass bed (6), where the gasification process reactions occur. The gases from the reactions flow downward until they find the holes below the grill (7), which give access to the gasifier jacket (8). Once in the jacket, the biomass gas flows upward to the outlet pipe (9), in contact with the pressure and temperature measuring instruments (10). Through the outlet pipe, the gases pass through the heat exchanger (11), where the temperature of the stream is reduced to values less than 30°C. In order to collapse the mist produced by the condensation of the tar and other vapors, the particle separator (sinuous section) is used (12).

In principle, the tar fraction in the gaseous mixture should settle when cooled and condensed. However, it has been experimentally observed that the condensate forms a suspension of very fine liquid particles that do not cluster so easily. For this reason, the separator (12) was installed with the function of recovering the tar as well as other condensable components.

The bubblers (14) were implemented to retain any traces of tar that were not retained by the separator (12). The bubblers were filled with isopropanol and subjected to a thermostatic bath at -5°C (13).

The accumulator vessel (*trap*) (15) is intended to contain solvent entrains which may possibly occur in the bubblers. After passing through the purification systems, the gas is analyzed (16). The gas volume is measured by means of a volume integrator (18) and its temperature measured by thermocouple (17).

In summary, during the gasification process, four products are generated: a) ash, by the base of the gasifier; b) condensates, by the base of the particle separator; c) tar solution in isopropanol, in the bubblers; and d) gases from the gasification of the wood, by the exit of the accumulator container (15).

The raw material to be carbonated was part of the finely chopped eucalyptus gallery as shown in Fig. 7.



**Fig. 7** – Minced eucalyptus branch used in gasification tests. **Source:** Authors' collection.

The characteristics of the material are presented in Table 3.

**Table 3** – Characteristics of the materials used in the study of gasification.

Average length (cm) (95% confidence)	1.66±0.16
Average diameter (cm) (95% confidence)	1.03±0.22
Apparent density (g/cm <sup>3</sup> )	0.349
Higher heating value [16]	4.501 kcal/kg
Elemental composition [17]	47.3%(C); 5.8%(H); 46.2%(O); 0.7%(N);

**Source:** Prepared by the authors.

The values shown in Table 3 were obtained by simple random sampling. The samples were 150 g of eucalyptus. The heating value and elemental composition were assumed to be constant, according to the literature [16, 17].

A volume integrator meter coupled to the inlet of the gasifier records the total volumetric amount of air (V) injected into the system. Once the volume of air, the ambient temperature (T) and the system pressure (P) are known, the mass of air ( $M_{ar}$ ) is calculated by Equation 22, according to the model for ideal gases.

$$M_{ar} = \overline{MM}_{ar} \frac{PV}{RT} \quad (22)$$

The constant  $\overline{MM}_{ar}$  is the average molar mass of air and  $R$  is the ideal gas constant.

The masses of ash, condensate, and biomass batch were determined by weighing to the nearest thousandths of a gram. Therefore, the only undetermined current is the current of the gas produced, whose mass can be calculated by difference, according to Equation 23:

$$M_{gas} = M_{biomass} + M_{air} - M_{ash} - M_{condensate} \quad (23)$$

At the end of the gasification, the amount of tar was determined. To this end, the amounts of tar present in the bubbler solution and in the condensers were collected and weighed.

The condensates received two phases, one organic and one aqueous. The aqueous phase was separated by decantation and reserved for treatment. The organic phase remained in the condenser.

Due to the cooling of the outlet stream, the tar contaminates the walls of all equipment and conduits downstream of the gasifier, requiring the cleaning of the gasifier using the isopropanol contained in the last two bubblers. The washing solutions were then pooled to the solution of the first bubbler, obtaining all the tar in isopropanol.

In this step, two main tar residues were obtained: in isopropanol and in aqueous solution. The fractions were weighed and filtered.

The recovery of the dissolved tar in both aqueous and organic media was done by roto-evaporation, using a 250 mL round bottom flask with 90 g of solution. In this process, the following steps were followed:

a) Step 1: evaporation was performed in a roto-evaporator with thermostatic bath. The bath temperature was set to 85°C, the pressure to 160 mmHg (abs), and the rotation was 60 rpm.

b) Step 2: it was visually observed the detachment of bubbles indicating the boiling of the solvent. After detachment, the first weighing of the flask was performed and the mass of the residue was determined by difference.

c) Step 3: the flask was repositioned in the roto-evaporator and evaporation continued for another 10 minutes, and then a new weighing was performed and the mass of tar residue was determined by difference.

d) Step 4: Step 3 was repeated until the mass of residue obtained did not vary by more than 2% between repetitions.

e) Step 5: the last mass obtained was considered as the final mass of tar residue.

Steps 1 to 5 were performed using representative samples of each solution, i.e., collected after perfect homogenization of the mixture.

The total mass of tar residue ( $M_{Alc}$ ) was calculated by Equation 24.

$$M_{Alc} = m_{Alc} \frac{M_s}{m_s} \quad (24)$$

Where  $M_s$  is the total mass of solution,  $m_s$  is the sample mass of solution used in roto-evaporation, and  $m_{Alc}$  is the residual sample mass of tar obtained at the end of evaporation.

The sum of the total residual mass of tar in the aqueous phase ( $M_{Alc(aq)}$ ) and the total residual mass of tar in the organic phase ( $M_{Alc(org)}$ ) provides the total mass of tar residue produced in the experiment ( $M_{Alc(total)}$ ), as indicated by Equation 25.

$$M_{Alc(total)} = M_{Alc(aq)} + M_{Alc(org)} \quad (25)$$

A Varian CP3800 chromatograph equipped with a TCD detector, Restek ShinCarbon ST 100/120 column (2 m long, 1 mm diameter) and helium as the carrier gas was used to determine the composition of the produced gas. To this end, a sample fraction of the synthesis gas was continuously directed to the chromatograph sampling valve, and the samples in this valve were taken every 20 minutes.

Chromatograph calibration was performed from mixtures of  $H_2$ ,  $CO$ ,  $CH_4$ , and  $CO_2$  gases of known concentration. Signal intensity was correlated with the known fraction of each component.

The molar amount of the components  $H_2$ ,  $CO$ ,  $CH_4$  and  $CO_2$  was calculated from the numerical integration of the product of the mole fraction of each component by the volume element. The mole fraction was obtained by chromatography, and the volume element was obtained by gasometer coupled to the outlet of the gasifier.

Thus, it was possible to analyze the concentration of  $H_2$ ,  $CO$ ,  $CH_4$  and  $CO_2$ .  $N_2$  was considered inert in the gasification process and was quantified based on the amount admitted at the reactor inlet. The water was condensed and determined by weighing. Oxygen was not quantified since the chromatographic column used does not allow the separation between nitrogen and oxygen. Thus, oxygen and other unidentified components were accounted for in a single fraction called "others". The air factor was calculated as the ratio between the amount of oxygen used in the gasification and the stoichiometric amount of oxygen for the complete combustion, both calculated for the same mass of fuel.

Three airflows were used in order to determine the effects of air intake variation in the gasification process. The average molar airflow rates used in the tests were  $5.62 \times 10^{-3}$  mol/s,  $7.03 \times 10^{-3}$  mol/s and  $9.96 \times 10^{-3}$  mol/s. To eliminate the effects of temperature and pressure variations, all flows were calculated on a molar basis and not on a volumetric basis.

### 3. Results and Discussion

#### 3.1 Air factor

It was observed that the air factor is not directly related to the molar airflow rate. That is, an increase in airflow rate does not significantly interfere with the air factor, since as the air flow rate increases, the experiment time decreases.

Fig. 8 illustrates the experimental behavior of the average biomass consumption rate as a function of the molar flow rate of air used.

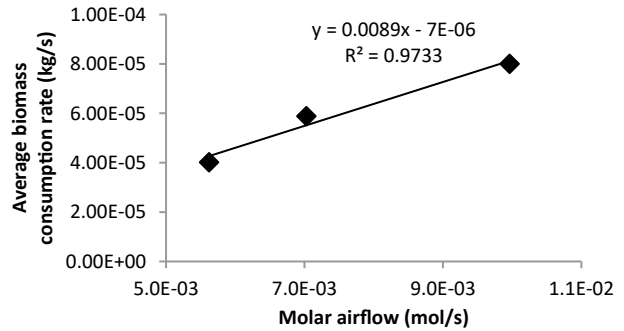


Fig. 8 – Average biomass consumption rate as a function of molar airflow. Source: Prepared by the authors.

As shown in Fig. 8, increasing the airflow rate, also increases the consumption of biomass, causing the  $O_2$  ratio provided by consumed biomass to remain constant, justifying the small variation of the air factor in relation to the airflow rate in the studied interval, since the mass ratio between stoichiometric  $O_2$  and the consumed biomass remains constant.

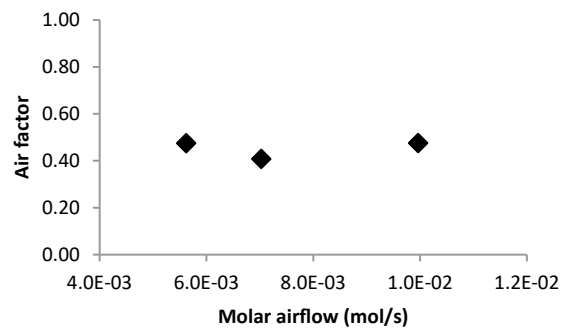


Fig. 9 – Air factor as a function of molar airflow. Source: Prepared by the authors.

Thus, the study of the gasification process took place in a narrow range of air factor, since this variable has little sensitivity to flow variation. In the tests performed, the highest value obtained was 0.48 and the lowest was 0.41, according to Fig. 9. Ma *et al.* [18] conducted studies in the range of 0.16 to 0.30, while Olgun, Ozdogan and Yinesor [7] managed to cover the range of 0.20 to 0.50, both for the air factor in gasifiers of the concurrent type in fixed bed.

The narrow range of air factors does not represent a negative factor, but rather a characteristic of the studied equipment.

### 3.2 Tar content

The tar production obtained was 12 to 24 g/m<sup>3</sup> of gas (at 25°C and 1 atm). Fig. 10 presents the values obtained experimentally for different values of airflow.

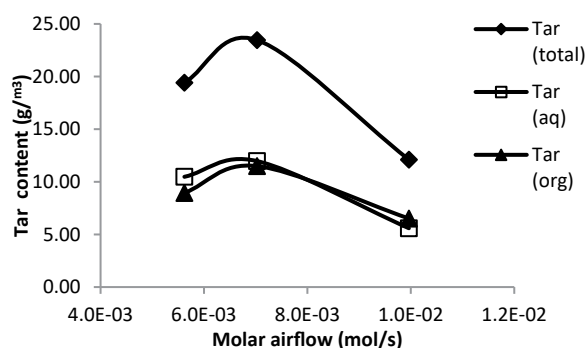


**Fig. 10** – Air factor as a function of molar airflow. **Source:** Prepared by the authors.

According to Stevens [19], concurrent gasifiers have a tar production in the range of 0.04 to 6 g/m<sup>3</sup> of tar. Thus, there is a high production of tar in relation to that mentioned in the literature. However, each gasifier can usually generate different results, especially those designed for bench. The existence of factors such as size, gasification technology, type of material used, gas used, use of steam, biomass extraction region, make the gasification process difficult to compare with the literature.

The high tar production in relation to the literature may be related to the reduced distance between the air injection point and the base of the biomass bed. Olgun, Ozdogan and Yinesor [7] positioned the injection points 250 mm above the base of the biomass bed, while Nisamaneenate *et al.* [20] used the 200 mm position. In the equipment used in this study, air was injected only 30 mm above the base of the biomass bed, providing shorter residence times in the bed.

### 3.3 Study of the thermal behavior of the bed

The gasifier was monitored with four thermocouples along the bed, arranged every 5 cm vertically, starting from the base. Temperature *versus* time graphs were converted to bed height *versus* time graphs. The temperature axis was divided into 5 regions, as follows:

- a) Region **a** (from 100 to 120 °C): range of water loss by drying;
- b) Region **b** (from 180 to 250°C): decomposition of extractives and the most reactive part of hemicellulose [21, 22];
- c) Region **c** (from 250 to 300°C): predominant degradation of cellulose, hemicellulose and part of lignin [22];
- (d) Region **d** (from 300 to 550 °C): degradation of lignin and residual parts of cellulose [19];
- e) Region **e** (from 900 to 1300°C): thermal degradation of tar [5, 9].

Thus, it is possible to verify which parts of the biomass bed are under the conditions of the regions **a**, **b**, **c**, **d** or **e** by means of the isotherms of 100, 120, 180, 250 and 550°C in relation to the bed height. The results obtained for such isotherms are presented in Fig. 11.

The downward movement of the biomass can cause, at times, the measured temperature to suffer large variations, given the possibility of no contact of the biomass with the thermocouple. Assuming, in this case, that the downward velocity of the bed is constant, the measurements above the dashed line in Fig. 11 are not representative of the bed.

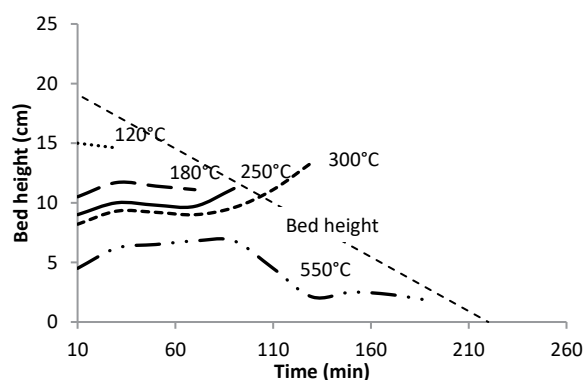


**Fig. 11** – Key isotherms for the pyrolysis of wood for the airflow of  $5.62 \times 10^{-3}$  mol/s. **Source:** Prepared by the authors.

In the test for airflow of  $5.62 \times 10^{-3}$  mol/s, it is verified that most of the bed had already gone through the drying process after 10 minutes, since practically the entire bed was already above  $120^\circ\text{C}$ . After 30 minutes, all the biomass was already fully dry. Pyrolysis occurs more intensely between the beginning of the experiment and 90 minutes – region between  $180$  and  $550^\circ\text{C}$  isotherms. From this period on, the fraction of the bed subjected to pyrolysis decreases due to the reduction in bed height.

The same analysis made for Fig. 11 in the airflow rate  $5.62 \times 10^{-3}$  mol/s was made for the other flow rates tested. In general, the same behavior profiles are observed in the tests. With the analysis of the isotherms for the three flow rates tested, Table 4 was constructed and, through this, a temporal distortion of the drying and pyrolysis effects was revealed for each airflow rate value.

**Table 4** – Time intervals characteristic of biomass bed degradation in airflow variation tests.

Lost Component or degraded	Flow rate (mol/s)		
	$5,62 \times 10^{-3}$	$7,03 \times 10^{-3}$	$9,96 \times 10^{-3}$
	Time Range (minutes)		
Water (drying)	0 to 30	0 to 30	0 to 10
Extractives	0 to 70	0 to 70	0 to 50
Hemicellulose + cellulose	0 to 90	0 to 70	0 to 50
Lignin	0 to 170	0 to 110	0 to 90
Experimental time	<b>0 to 220</b>	<b>0 to 150</b>	<b>0 to 130</b>

Source: Prepared by the authors.

Based on the temperature ranges described, it is possible to make two observations. First, from the initial minutes of the experiment, the entire bed is already in the drying process. Most of the biomass moisture is eliminated already in the first 30 minutes of the experiment. Second, the maximum bed temperature – measured at the bottom – rarely reaches the thermal decomposition range of tar, indicating the formation of high amounts of tar in all three experiments.

### 3.4 Gas composition

Fig. 12 presents the compositions on a dry basis of the gas produced in the gasification system.

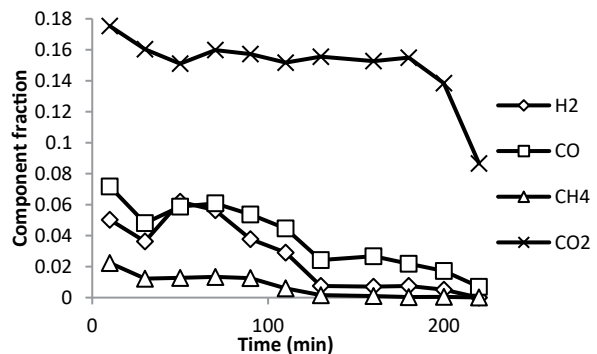


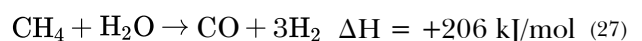
**Fig. 12** – Gas composition for the molar airflow rate of  $5.62 \times 10^{-3}$  mol/s. Source: Prepared by the authors.

For the organization of the work, three characteristic thermal periods were named for batch or semi-batch gasification: (1) drying period, (2) pyrolysis period and (3) coal gasification period. These periods were defined by analyzing the temperature profiles using isotherms (Fig. 11).

In general, the experiments revealed a common pattern among themselves for the production of  $\text{H}_2$  and  $\text{CO}$ . Observing the behavior of the composition of the gas produced and comparing with the analysis of the thermal profiles, it is possible to note that there is a correlation between the thermal behavior of the bed and the composition of gas produced.

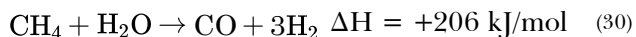
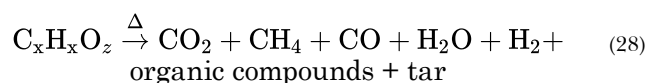
The drying period and the pyrolysis period tend to generate high levels of  $\text{CO}$  and  $\text{H}_2$ , while the coal gasification period generates more  $\text{CO}$  and  $\text{CO}_2$ .

In the initial minutes of gasification, the  $\text{H}_2$  and  $\text{CO}$  fractions are higher. It is reasonable to assume that the increased concentration of these species is the result of the release of water in the bed due to the drying process. This greater amount of water favored the steam reforming reactions inside the gasifier. It is worth remembering that  $\text{CO}$  can also be produced in processes other than steam reforming, so a greater availability of water will not always lead to greater  $\text{CO}$  production. Equations 26 and 27 are favored by the presence of water:

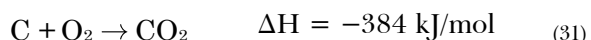


The effect of drying on the production of H<sub>2</sub> and CO, however, occurs only in the initial moments of the experiments. In the case of the highest airflow rate studied (9.96×10<sup>-3</sup> mol/s), this effect is not even detected, since drying occurs even before the first gas sampling.

A peak production of H<sub>2</sub> and CO is observed from the end of drying to the end of pyrolysis. In this period, the higher production of H<sub>2</sub> and CO is associated with the very phenomenon of pyrolysis (Equation 28) and the steam reforming reactions that are made possible by the release of water by pyrolysis, as shown by Equations 29 and 30.



Finally, when complete pyrolysis of the biomass occurs, only coal remains, which continues in the gasification process. Due to its high carbon content, coal mainly generates CO and CO<sub>2</sub> as products when dry air is used for gasification. Thus, at this stage, the most important reactions are those of carbon combustion (Equations 31 and 32) and the Boudouard reaction (Equation 33).



In the three experiments, the CO<sub>2</sub> fraction remained approximately constant with the test time. Small reductions in CO<sub>2</sub> content occurred as a function of dilution by CO and H<sub>2</sub>. In addition, the CO<sub>2</sub> fraction was not affected by the change in airflow, remaining between 15% and 16% for all airflows used.

The amount of methane remained below 2% most of the time for all airflows tested. It is difficult to assess by which route methane is produced, because this gas is involved in many reactions such as combustion, steam reforming, dry reforming, wood

pyrolysis, methanation etc. However, the reduction in methane content is notorious as the bed reaches the coal gasification period, certainly due to the scarcity of the hydrogen element in the bed material (Table 5).

**Table 5** – Global composition of the gas produced in the airflow variation tests.

	Molar airflow (mol/s)		
	5.62×10 <sup>-3</sup>	7.03×10 <sup>-3</sup>	9.96×10 <sup>-3</sup>
<b>Air factor</b>	0.47	0.41	0.48
<b>H<sub>2</sub></b>	2.85%	4.38%	5.36%
<b>CO</b>	4.10%	6.46%	6.73%
<b>CH<sub>4</sub></b>	0.78%	0.96%	0.81%
<b>CO<sub>2</sub></b>	15.27%	15.32%	12.60%
<b>N<sub>2</sub></b>	71.35%	66.86%	73.20%
<b>Other</b>	5.64%	6.02%	1.30%

Source: Prepared by the authors.

The integration of the amount produced of each component from the initial moment to the final moment of each experiment allowed to calculate the composition of the gas produced, as shown in Table 5.

Table 5 shows that, for the airflow rate equal to 9.96×10<sup>-3</sup> mol/s, higher molar concentrations of CO and H<sub>2</sub> are produced. At this flow rate, it reaches a maximum of 12.8% H<sub>2</sub> and 14.8% CO and average values of 5.36% H<sub>2</sub> and 6.73% CO.

### 3.5 Energy performance

Using the gasifier at its maximum biomass load and the airflow rate at 7.03×10<sup>-3</sup> mol/s, the higher heating value (HHV) of the gas was 1,617 kJ/m<sup>3</sup>, and the lower heating value (LHV) was 1,491 kJ/m<sup>3</sup>. Ma *et al.* [18] obtained a gas with the LHV of 4,440 kJ/m<sup>3</sup> for the gasification of rice husks, and Altafini, Wander and Barreto [23] were able to produce synthesis gas with the HHV of 5,276 kJ/m<sup>3</sup>. Using the same gasifier applied in this work, França [24] obtained LHV of 1,167 kJ/m<sup>3</sup> for the gasification of açai stones.

This significant difference was expected due to the high concentration of CO<sub>2</sub> in the gas produced in this work, as well as the high thermal losses observed for a gasifier with high surface area to volume ratio, which is typical of small equipment.

## 4. Conclusion

The instrumental arrangement for measuring biomass bed temperatures, although very simple and inexpensive, allowed the mapping of the biomass bed through the most important isotherms in the pyrolysis and gasification processes. Thus, it was possible to evaluate and detect the phenomena occurring in the bed, either as a function of time or as a function of longitudinal position in the bed.

The air factor showed little sensitivity to molar airflow variation for the range of  $5.62 \times 10^{-3}$  to  $9.96 \times 10^{-3}$  mol/s. Consequently, flow variations within this range resulted in a very narrow air factor range.

For all experiments, the drying period and the pyrolysis period tend to generate high levels of CO and H<sub>2</sub>, while the carbon gasification period mainly

generates CO and CO<sub>2</sub>. Drying offers a greater amount of water, which intensifies the steam reforming reactions inside the gasifier. Pyrolysis is responsible for the increase in the production of H<sub>2</sub> and CO, either by the direct production of these components or by the steam reforming reactions that are made possible by the release of water in this process.

In view of the above, it is concluded that the tested unit, supported by its instrumentation, served to study the gasification process. The gasifier effectively produced syngas with all the components expected, presenting values comparable to those in the literature. The equipment used ensured the measurement of all quantities and parameters necessary for the study of the process and allowed the mass and energy balances to be performed successfully.

## References

- [1] LEITE, R. C. C.; LEAL, M. R. L. V. O biocombustível no Brasil. *Novos Estudos*, n. 78, p. 15–21, 2007. <https://doi.org/10.1590/S0101-33002007000200003>.
- [2] SILVA, G. A.; CARMO, J. S.; SANTOS, M. S. M.; BATISTOTE, M. Biomassa: conhecer para transformar. *Revista Conexão UEPG*, v. 13, n. 3, p. 462–473, 2017. <https://doi.org/10.5212/Rev.Conexao.v.13.i3.0009>.
- [3] NASCIMENTO, R. S.; ALVES, G. M. Fontes alternativas e renováveis de energia no Brasil: métodos e benefícios ambientais. In *XX Encontro Latino Americano de Iniciação Científica; XVI Encontro Latino Americano de Pós-Graduação; VI Encontro de Iniciação à Docência*. São José dos Campos: Univap, 2016. Available at: [http://www.inicepg.univap.br/cd/INIC\\_2016/anais/arquivos/0859\\_1146\\_01.pdf](http://www.inicepg.univap.br/cd/INIC_2016/anais/arquivos/0859_1146_01.pdf). Accessed on: Dec. 13, 2020.
- [4] SOUZA, R. C. R.; SANTOS, E. C. S. Incentivos ao uso de biomassa para geração de eletricidade na Amazônia. In *III Congresso Brasileiro de Regulação dos Serviços Públicos Concedidos*. Brasília, DF: ABAR, 2003.
- [5] LORA, E. E. S.; ANDRADE, R. V.; MARTÍNEZ ÁNGEL, J. D.; LEITE, M. A. H.; ROCHA, M. H.; SALES, C. A. V. B. et al. Gaseificação e pirólise para a conversão da biomassa em eletricidade e Biocombustíveis. In LORA, E. E. S.; VENTURINI, O. J. (ed.). *Biocombustíveis*. Rio de Janeiro: Interciência, 2012. p. 411–498.
- [6] MÜLLER, R.; VON ZEDTWITZ, P.; WOKAUNA, A.; STEINFELD, A. Kinetic investigation on steam gasification of charcoal under direct high-flux irradiation. *Chemical Engineering Science*, v. 58, no. 22, p. 5111–5119, 2003. <https://doi.org/10.1016/j.ces.2003.08.018>.
- [7] OLGUN, H.; OZDOGAN, S.; YINESOR, G. Results with a bench scale downdraft biomass gasifier for agricultural and forestry residues. *Biomass and Bioenergy*, v. 35, n. 1, p. 572–580, 2011. <https://doi.org/10.1016/j.biombioe.2010.10.028>.
- [8] DEVI, L.; PTASINSKI, K. J.; JANSSEN, F. J. J. G. A review of the primary measures for tar elimination in biomass gasification processes. *Biomass and Bioenergy*, v. 24, n. 2, p. 125–140, 2003. [https://doi.org/10.1016/S0961-9534\(02\)00102-2](https://doi.org/10.1016/S0961-9534(02)00102-2).
- [9] RICHARDSON, Y.; BLIN, J.; JULBE, A. A short overview on purification and conditioning of syngas produced by biomass gasification: catalytic strategies, process intensification and new concepts. *Progress in Energy and Combustion Science*, v. 38, n. 6, p. 765–781, 2012. <https://doi.org/10.1016/j.pecs.2011.12.001>.
- [10] MILNE, T. A.; EVANS, R. K.; ABATZOGLOU, N. Biomass gasifier “tars”: their nature, formation, and conversion. Golden, CO: National Renewable Energy Laboratory, 1998. Available at: <http://www.nrel.gov/docs/fy99osti/25357.pdf>. Accessed on: Nov. 27, 2014.

- [11] HIMMELBLAU, D. M.; RIGGS, J. B. Engenharia Química: princípios e cálculos. 7. ed. Rio de Janeiro: LTC, 2006.
- [12] FORTUNATO, B.; BRUNETTI, G.; CAMPOREALE, S. M.; TORRESI, M.; FORNARELLI, F. Thermodynamic model of a downdraft gasifier. *Energy Conversion and Management*, v. 140, p. 281–294, 2017. <https://doi.org/10.1016/j.enconman.2017.02.061>
- [13] QUITETE, C. P. B.; SOUZA, M. M. V. M. Remoção do alcatrão de correntes gaseificação de biomassa: processos e catalisadores. *Química Nova*, v. 37, n. 4, p. 689–698, 2014. <https://doi.org/10.5935/0100-4042.20140110>.
- [14] FOEKEL, C. Utilização da biomassa do eucalipto para produção de calor, vapor e eletricidade. In *Eucalyptus Online Book*. *Eucalyptus Online Book & Newsletter*, 2016. Available at: <http://www.eucalyptus.com.br/>. Accessed on: Dec. 13, 2020.
- [15] INDÚSTRIA BRASILEIRA DE ÁRVORES. Relatório 2019. Indústria Brasileira de Árvores. Brasília, DF, 2019. Available at: <https://iba.org/datafiles/publicacoes/relatorios/iba-relatorioanual2019.pdf>. Accessed on: Dec. 13, 2020.
- [16] QUIRINO, W. F.; VALE, A. T.; ANDRADE, A. P. A.; ABREU, V. L. S.; AZEVEDO, A. C. S. Poder calorífico da madeira e de materiais ligno-celulósicos. *Revista da Madeira*, n. 89, p. 100–06, 2005.
- [17] ZANUNCIO, A. J. V.; NOBRE, J. R. C.; MOTTA, J. P.; TRUGILHO, P. F. Química e colorimetria da madeira de *Eucalyptus grandis* W. Mill ex Maiden termorretificada. *Revista Árvore*, v. 38, n. 4, p. 765–770, 2014. <https://doi.org/10.1590/S0100-67622014000400020>.
- [18] MA, Z.; YE, J.; ZHAO, C.; ZHANG, Q. Gasification of rice husk in a downdraft gasifier: the effect of equivalence ratio on the gasification performance, properties, and utilization analysis of byproducts of char and tar. *BioResources*, v. 10, n. 2, p. 2888–2902, 2015. <https://doi.org/10.15376/biores.10.2.2888-2902>.
- [19] STEVENS, D. J. Hot gas conditioning: recent progress with larger-scale biomass gasification systems – Update and summary of recent progress. Golden CO: National Renewable Energy Laboratory, 2001.
- [20] NISAMANEENATE, J.; ATONG, D.; SORNKADE, P.; SRICHAROENCHAIKUL, V. Fuel gas production from peanut shell waste using a modular downdraft gasifier with the thermal integrated unit. *Renewable Energy*, v. 79, p. 45–50, 2015. <https://doi.org/10.1016/j.renene.2014.09.046>.
- [21] POLLETO, M.; ZATTERA, A. J.; SANTANA, R. M. C. Thermal decomposition of wood: kinetics and degradation mechanisms. *Bioresource Technology*, v. 126, p. 7–12, 2012.
- [22] SOARES, V. C. Comportamento térmico, químico e físico da madeira e do carvão de *Eucalyptus urophylla* X *Eucalyptus Grandis* em diferentes idades. Thesis (Doctorate in Science and Technology of Madeira) – Federal University of Lavras, Lavras, 2011.
- [23] ALTAFINI, C. R.; WANDER, P. R.; BARRETO, R. M. Prediction of the working parameters of a wood waste gasifier through an equilibrium model. *Energy, Conversion and Management*, v. 44, n. 17, p. 2763–2777, 2003.
- [24] FRANÇA, R. R. Desenvolvimento de unidade de gaseificação de bancada para produção de gás de síntese a partir de biomassa. Dissertation (Master in Physicochemistry) – Military Institute of Engineering, 2017.